Nonlinear Analysis of Noise in Static and Dynamic Translinear Circuits

Jan Mulder, Michiel H. L. Kouwenhoven, *Member, IEEE*, Wouter A. Serdijn, *Member, IEEE*, Albert C. van der Woerd, and Arthur H. M. van Roermund, *Senior Member, IEEE*

***Abstract*—For translinear filters, or log-domain filters, calculation of the maximal signal-to-noise-ratio, an important filter specification, is not trivial, due to the inherent companding behavior and the nonstationary nature of the transistor noise sources. To address this issue, a nonlinear noise analysis method is proposed. Based on large-signal calculations, expressions for the first-order noise and signal–noise intermodulation terms are computed. The procedure is generally applicable both to static and dynamic translinear circuits, as illustrated by a number of generic examples.**

***Index Terms*—Companding, log-domain, noise, translinear.**

I. Introduction

A PROMISING approach to meet the challenges the area of analog integrated continuous-time filters is facing, due to ever more restrictive low-voltage and low-power demands, is formed by the recently introduced class of translinear (TL) filters [1]–[7]. translinear filters are based on the "dynamic translinear principle" [8], a generalization of the conventional translinear principle [9], which we will here refer to as the "static translinear principle." Whereas conventional TL circuits can be used to implement various linear and nonlinear *static* transfer functions, dynamic TL circuits implement a wide variety of *dynamic* functions, described by differential equations (DE). Both linear DE's, i.e., filters [1]–[7], and nonlinear DE's, e.g., oscillators [10], [11], adaptive filters [12], PLL's [13], [14], and RMS-DC converters [8], [15] can be realized.

The dynamic range (DR) and the maximal signal-to-noise ratio (SNR) are important specifications for analog filters. Determination of the DR of a TL filter is quite easy, if it is defined as the ratio of the maximal signal level the filter can handle and the absolute noise floor. The maximal signal level is determined by a specified maximal distortion level, for harmonic or intermodulation distortion. The absolute noise floor is defined as the amount of noise generated within the filter in the absence of any input signals. Without any signals present, the equivalent input or output noise can be calculated using a small-signal equivalent model of the TL filter. Hence, only linear noise equations have to be solved to calculate the DR.

Manuscript received July 31, 1999; revised May 30, 1998.

The authors are with the Electronics Research Laboratory/DIMES, Faculty of Information Technology and Systems, Delft University of Technology, Delft, The Netherlands.

Publisher Item Identifier S 1057-7130(99)01769-3.

Calculation of the SNR, defined here as the ratio of the signal power and the noise power *at the same instant*, is much more difficult for TL filters, and, in fact, for all companding or nonlinear systems. Since TL circuits are explicitly based on the exponential behavior of the transistor, they are inherently instantaneous companding. Therefore, although the over-all transfer function is linear, even for large signals, these circuits are internally nonlinear. This results in intermodulation of the signals being processed with noise and interference [16]–[21].

The situation is even complicated by the fact that the internal noise sources are generally nonstationary. The transistor currents in a TL filter are signal-dependent. Thus, the transistor shot noise sources are modulated by the signals being processed [16], [22], [23].

A number of noise analysis methods for static and dynamic TL circuit have been proposed previously [20], [24], [25]. However, since the approach used in these publications is quasilinear and quasistationary, these methods cannot adequately account for the nonlinear and nonstationary properties of noise in TL circuits. Note that also most circuit simulators do not facilitate nonlinear noise analysis.

In this paper, a generally applicable nonlinear analysis method for noise bin TL circuits is proposed. The presented technique enables calculation of the first-order noise and signal–noise intermodulation, both in static and dynamic TL circuits. A current-mode approach is followed, since TL circuits can be described most elegantly in terms of currents [9], [25], [26]. Another advantage of this approach is that the existing theory on static TL circuits, see, e.g., [25] and [27], directly becomes available to the analysis and synthesis of dynamic TL circuits [26], [28], [29]. The noise behavior of the related class of $\sqrt{}$-domain filters [30], [31], based on the MOS transistor in the strong inversion region, is beyond the scope of this article. The interested reader is referred to [16].

In Section II the underlying principles of both static and dynamic TL circuits are reviewed. Section III considers the relevant noise sources of the bipolar transistor and the MOS transistor in the subthreshold region. Section IV describes the principles of the nonlinear noise analysis method. Its application is illustrated for some generic examples of static and dynamic TL circuits in Sections V and VI, respectively. The examples cover linear and nonlinear TL circuits, operated in class A and class AB.

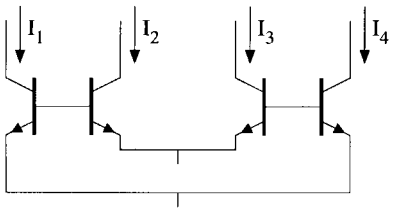

Fig. 1. Four-transistor translinear loop.

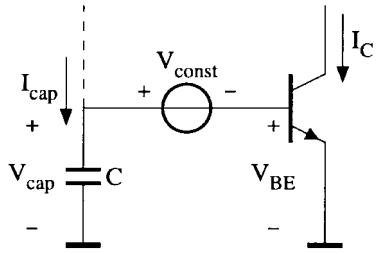

Fig. 2. Principle of dynamic translinear circuits.

II. Translinear Principles

Translinear circuits can be divided into two major groups: static and dynamic TL circuits. The first group can be applied to realize a wide variety of linear and nonlinear static transfer functions. All kinds of frequency-dependent functions can be implemented by circuits of the second group. The underlying principles of static and dynamic TL circuits are reviewed in this section.

A. Static Translinear Principle

Translinear circuits are based on the exponential relation between voltage and current, characteristic for the bipolar transistor and the MOS transistor in the weak inversion region. The collector current I_C of a bipolar transistor in the active region is given by

$$I_C = I_s e^{V_{\rm BE}/U_T} \tag{1}$$

where all symbols have their usual meaning.

The TL principle applies to loops of semiconductor junctions. A TL loop is characterized by an even number of junctions [9], [25], [32]. The number of devices with a clockwise orientation equals the number of counter-clockwise oriented devices. An example of a four-transistor TL loop is shown in Fig. 1. It is assumed that the transistors are somehow biased at the collector currents I_1 through I_4, and have equal emitter areas. When all devices operate at the same temperature, this yields the familiar representation of TL loops in terms of products of currents

$$I_1 I_3 = I_2 I_4. \tag{2}$$

This generic TL equation is the basis for a wide variety of static electronic functions, which are theoretically temperature and process independent.

B. Dynamic Translinear Principle

The static TL principle is limited to frequency-independent transfer functions. By admitting capacitors in the TL loops, the TL principle can be generalized to include frequency dependent transfer functions. The term "dynamic translinear" was coined in [8] to describe the resulting class of circuits. In contrast to other names proposed in literature, such as "log-domain" [1], "companding current-mode" [2], "exponential state-space" [33], this term emphasizes the TL nature of these circuits.

The dynamic TL principle can be explained with reference to the subcircuit shown in Fig. 2. Using a current-mode approach, the capacitance current $I_{\rm cap}$ can be expressed in terms of the collector current I_C, the capacitance C, and the thermal voltage U_T as

$$I_{\rm cap} = C U_T \frac{\dot{I}_C}{I_C} \tag{3}$$

where the dot represents differentiation with respect to time. Obviously, the DC voltage source V_{const} does not affect $I_{\rm cap}$. More insight is gained by slightly rewriting (3) as

$$C U_T \dot{I}_C = I_{\rm cap} \cdot I_C. \tag{4}$$

This equation directly states the "dynamic translinear principle": *A time derivative of a current can be mapped onto a product of currents*. At this point, the conventional TL principle comes into play, for, the product of currents on the right-hand side (RHS) of (4) can be realized very elegantly by means of this principle. Thus, the implementation of (part of) a DE becomes equivalent to the implementation of a product of currents.

The dynamic TL principle can be used to implement a wide variety of DE's, describing frequency-dependent signal processing functions. For example, linear filters are described by linear DE's. Examples of nonlinear DE's are harmonic [10], [11] and chaotic oscillators, PLL's [13], [14] and RMS-DC converters [8], [15].

III. Transistor Noise Sources

Two types of transistors are applicable to the design of TL circuits. These are the bipolar transistor and the MOS transistor operated in the subthreshold region. In this section, the noise sources of these transistors are shortly reviewed and, their relative influence in TL circuits is discussed.

The convention used throughout the paper is to preserve the lower case letter "i" for noise currents and the upper case letter "I" for signal currents. Indices are used to distinguish between different noise or signal currents.

A. Bipolar Transistor

The noise behavior of the bipolar transistor is characterized mainly by four statistically independent noise sources: collector shot noise, base shot noise, flicker noise, and thermal base resistance noise.

The collector shot noise is represented by a noise current source i_C connected between the collector and emitter terminals. The double-sided power spectral density function S_{i_C} of i_C is white, and equals

$$S_{i_C}(\omega, t) = q I_C(t) \tag{5}$$

where q is the unity charge.

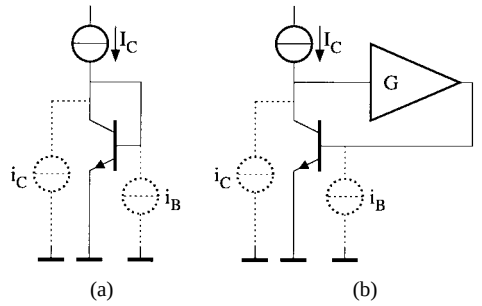

Fig. 3. Biasing of a transistor in a translinear circuit using (a) a diode connection or (b) an amplifier.

The base shot noise is represented by a noise current source i_B connected between the base and emitter terminals. The double-sided power spectral density function S_{i_B} of this source is also white, and equals

$$S_{i_B}(\omega, t) = qI_B(t). \tag{6}$$

In TL circuits, the influence of the base shot noise is often negligible in comparison to the collector shot noise. This follows by evaluation of the limited number of schemes available to force the collector currents. Usually, the collector currents are forced through the transistors using either diode-like connections or (simple) amplifier implementations, as illustrated in Fig. 3. In the diode connected transistor, shown in Fig. 3(a), i_B and i_C are connected in parallel. The noise power of i_B is β_F times smaller than the noise power of i_C, and thus negligible for sufficiently large values of β_F. In Fig. 3(b), the amplifier further reduces the influence of i_B: when transformed to the collector terminal, i_B is divided by the current gain G of the amplifier. This amplifier is often implemented by a CC stage, which possibly is another transistor in the TL loop, or a differential pair.

In fact, i_B can become important only when large magnitude differences, of at least a factor β_F, exist between the collector currents. In such cases, however, the base currents are likely to introduce large errors that have to be eliminated. If amplifiers are used to this end, the influence of i_B is likewise eliminated. Only when feed-forward error compensation methods, instead of negative feedback, are used i_B can be come important, since it is multiplied by β_F when transformed to the collector terminal.

The $1/f$ noise, or flicker noise, which is the product of a process-dependent noise mechanism, is also represented by a noise current source between the base and emitter terminals. For dc base currents, the power spectral density of this noise, given by

$$S_{i_B f}(\omega) = qI_B \frac{2\pi f_l}{\omega} \tag{7}$$

is characterized by a frequency f_l, at which it equals the base shot noise spectral density (6). The relative importance of the $1/f$ noise decreases with a decreasing dc current I_B, since f_l decreases with I_B [34]. Since in common bipolar IC processes, f_l is quite low, typically a few hertz, $1/f$ noise is usually negligible compared to the base and collector shot noise. In some TL circuits, signal $\times$ noise intermodulation may cause the flicker noise to be copied from low frequencies to other frequency bands, due to a time-dependent base current.

In noise analyzes, the collector and base currents are usually approximated as being dc currents. All corresponding shot noise sources are thus stationary. For TL circuits, however, this approximation is not accurate. There, the transistor currents are often strongly signal-dependent, causing principally non-stationary shot noise sources. This explains the time variable t in (5) and (6).

The thermal noise v_{R_B}, generated by the base resistance R_B of the bipolar transistor, has a white power spectral density S_{R_B} given by

$$S_{R_B}(\omega) = 2kTR_B \tag{8}$$

where k is Boltzman's constant and T is the absolute temperature. Due to the preference for a current-mode approach, the noise voltage v_{R_B} has to be transformed to a noise current source i_{R_B} connected in parallel with i_C.[1] Since $v_{R_B} \ll U_T$, the (small-signal) transconductance $g_m = I_C/U_T$ can be used for this transformation. The signal-dependence of I_C can generally not be neglected in TL circuits. Therefore, the power spectral density $S_{i_{R_B}}$ of the transformed current source i_{R_B} is found to be

$$S_{i_{R_B}}(\omega, t) = qI_C(t)\frac{2R_B I_C(t)}{U_T}. \tag{9}$$

Comparing (5) and (9) shows that v_{R_B} is negligible when the transistor is operated at low current levels, where $I_C \ll \frac{1}{2}U_T/R_B$, while it is the dominant noise source at high current levels, where $I_C \gg \frac{1}{2}U_T/R_B$. At moderate current levels, both i_C and i_{R_B} have to be included in the analysis.

An indication of the maximal SNR of a TL circuit can be derived from the SNR of a single bipolar transistor. The signal power processed by a single transistor is proportional to the square of I_C. For simplicity, here, we regard the DC value of I_C as being the processed signal, in which case all noise sources become stationary. Dividing this by the noise power in an equivalent noise bandwidth B (in hertz) yields the SNR of a single bipolar transistor

$$\text{SNR} = \frac{I_C}{2qB(1 + 2R_B I_C/U_T)}. \tag{10}$$

Fig. 4 plots (10) for $R_B = 600\ \Omega$ and $B = 1$ MHz. At low current levels, the SNR increases linearly proportional to I_C, due to i_C, while at high current levels, it saturates to 78 dB, due to i_{R_B}. This saturation level follows from the asymptote

$$\lim_{I_C \to \infty} \text{SNR} = \frac{U_T}{4qR_B B}. \tag{11}$$

A TL circuit consists of one or several TL loops [25]. Each of these loops can more or less be regarded as being a cascade of transistors. According to (10), the SNR of such a loop is

[1] In principle, this transformation of v_{R_B} yields besides a noise current source between the collector and emitter terminals also a noise voltage source in series with the collector terminal. However, the influence of the latter on I_C is negligible, due to the high transistor output impedance.

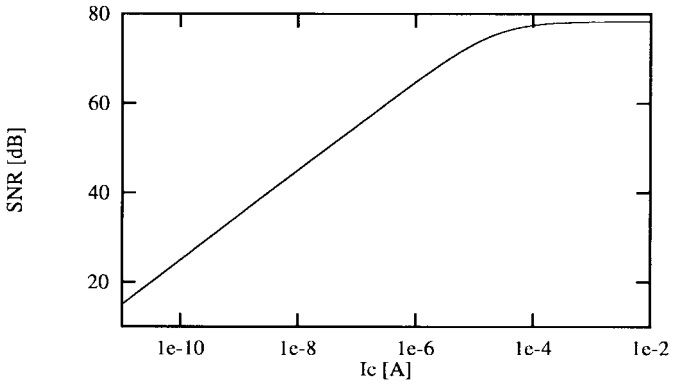

Fig. 4. Signal-to-noise-ratio of a bipolar transistor, for $R_B = 600\ \Omega$ and $B = 1$ MHz.

thus limited by the transistor that has the lowest ratio of the collector current and the equivalent noise bandwidth. The SNR of a single-loop TL circuit is proportional to (and in the order of) (11), as discussed in subsequent sections.

B. MOS Transistor

The noise of an MOS transistor in the subthreshold region, where the V–I relation is exponential, is basically modeled by one noise current source, connected between the source and drain terminals. The power spectral density S_{i_d} of its shot noise component equals [35]

$$S_{i_d}(\omega, t) = q[I_F(t) + I_R(t)] \tag{12}$$

where the forward and reverse components of the drain current $I_{DS} = I_F - I_R$ in weak inversion equal [36]–[38]

$$I_F = I_o e^{V_G/nU_T} e^{-V_S/U_T} \tag{13}$$

$$I_R = I_o e^{V_G/nU_T} e^{-V_D/U_T} \tag{14}$$

and all symbols have their usual meaning. In the saturation region, the most prevalent region for TL circuits, $V_D \gg U_T$ and S_{i_d} simplifies to $S_{i_d} = qI_{DS}(t)$ [39].

In addition to this white shot noise, the MOS transistor also exhibits $1/f$ noise. However, it can be shown that $1/f$ noise is negligible at low current levels [39], the region used in MOS-TL circuits.

IV. Noise Analysis Method

Due to fact that TL circuits use the exponential nature of the transistor in a very specific way, their nonlinear properties can be made more explicit. Basically, three different appearances of the exponential device characteristics can be distinguished. First, the multiplication of collector currents, see (2), and the transformation of noise voltage sources into noise current sources, see (9), introduce signal $\times$ noise intermodulation. Second, due to the time-dependent collector currents, the noise current sources are generally nonstationary. Finally, the inclusion of capacitances in DTL circuits may result in dynamically nonlinear transfers [40].

The objective of the nonlinear noise analysis method is to determine the equivalent output noise of a TL circuit due to internal noise production. This is achieved by application of the following general sequence of steps.

A. TL Equations in the Presence of Noise

The first step is the determination of the TL equations in the presence of noise. To this end, the main noise sources of each transistor are added to the circuit. For example, Fig. 5 depicts the inclusion of collector shot noise current sources and thermal base resistance voltage noise sources in the second-order TL loop of Fig. 1. All transistors are assumed to be biased at the currents I_1 through I_4.

Since a TL analysis is elaborated in the current-domain, the thermal noise voltage sources v_5–v_8 have to be transformed into noise current sources through application of (9). In general, this transformation introduces signal–noise intermodulation, since v_5–v_8 are multiplied by a time-dependent collector current $I_C(t)$. Only when the TL loop contains a transistor that is biased at a constant current, this intermodulation can be circumvented. Since the junctions in a TL loop are series connected, v_5–v_8 can be combined into a single noise source v_n. This resulting noise source can move freely through the TL loop and transformed into a current source i_n by application of (9) to an arbitrary transistor in the loop. Obviously, a transistor biased at a constant current, having a constant g_m, yields the simplest result.

Therefore, the noise currents i_1–i_4 that accompany the collector currents I_1–I_4, may, besides the (nonstationary) collector shot noise, also be thought to include the transformed thermal voltage noise and possibly other noise contributions. The total collector current that flows through transistor number n in the circuit thus consists of a signal component I_n and a noise component i_n. The TL equation of the circuit in Fig. 5 is then obtained by replacement of the collector currents I_n in the noise-free TL (2) by the noisy currents $I_n + i_n$. This yields

$$(I_1 + i_1)(I_3 + i_3) - (I_2 + i_2)(I_4 + i_4) = 0. \tag{15}$$

Such a TL decomposition, containing both signals and noise, is the basis for the nonlinear noise analysis. An important advantage is that it allows (an approximate) evaluation of the noise behavior in an early phase of the synthesis path, long before the circuit design is completed.

B. Input–Output Equation Including First-Order Noise

The second step is the determination of the circuit's input–output relation, including first-order noise and signal $\times$ noise intermodulation terms. Elaboration of the decomposition in (15) yields a second-order polynomial in I_1–I_4 and i_1–i_4. In general, an nth-order polynomial is obtained for an nth-order TL loop. Each separate term of the expanded decomposition comprises products of signal and/or noise currents. As long as the noise is much smaller than the signals, products of noise currents are negligible. Hence, only those product terms containing at most one noise component, i.e., first-order noise or signal–noise intermodulation, are relevant. For (15) this yields

$$I_1 I_3 - I_2 I_4 + I_1 i_3 + I_3 i_1 - I_2 i_4 - I_4 i_2 = 0. \tag{16}$$

The input–output relation follows by solving the expanded decomposition for the output current I_{out}, which is one of the currents I_n, as a function of the input current I_{in} and the noise

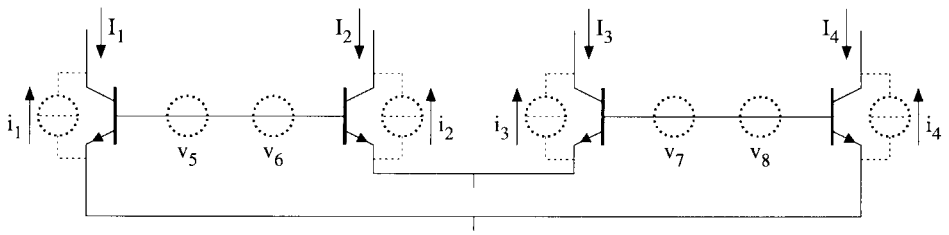

Fig. 5. Translinear loop in the presence of noise.

currents i_n. The resulting expression is a polynomial, a rational function or an expression containing nth-order root functions. Since only first-order noise components are of interest for signals that are much larger than the noise, this expression can be approximated by a first-order, n-dimensional Taylor series with respect to all noise sources i_n. This yields I_{out} expressed as a function of I_{in} and all first-order noise and signal–noise components.

Note that this approach eliminates all interactions between the noise sources i_n, while the signal-dependence of the noise is preserved. The circuit response to all independent noise sources can therefore be calculated individually and added afterwards.

C. Autocorrelation and Power Spectral Density

The third step is the determination of the autocorrelation and power spectral density of I_{out}. These are easily obtained when I_{out} is divided into three mutually uncorrelated components. Let $\vec{s}(t)$ symbolize the vector of all independent input signals applied to the circuit and $\vec{n}(t)$ the vector of all noise currents i_n. Note that $\vec{n}$ is statistically *dependent* on $\vec{s}$ when it includes nonstationary shot noise. Then, I_{out} comprises a deterministic component $\mathcal{C}(t)$, a signal component $\mathcal{S}(t)$, and a noise component $\mathcal{T}(t)$ that are mutually uncorrelated [41]

$$\mathcal{C}(t) = e[I_{\text{out}}(t)]_{\vec{s},\vec{n}} \tag{17a}$$

$$\mathcal{S}(t) = e[I_{\text{out}}(t)|\vec{s}(t)]_{\vec{n}} - \mathcal{C}(t) \tag{17b}$$

$$\mathcal{T}(t) = I_{\text{out}}(t) - \mathcal{S}(t) - \mathcal{C}(t) \tag{17c}$$

where $E[.]$ denotes a statistical expectation. In principle, $\mathcal{T}(t)$ can be separated into a signal-independent noise component $\mathcal{N}(t)$ and a signal-dependent noise component $\mathcal{I}(t)$ [41]. In TL circuits, however, this is generally inconvenient due to the dependence of $\vec{n}$ on $\vec{s}$.

As a result, the autocorrelation of I_{out}, $R_{I_{\text{out}}}(\tau, t)$ also consists of the autocorrelations of these three components. The same holds for the power density spectrum $S_{I_{\text{out}}}(\omega, t)$, the Fourier transform of $R_{I_{\text{out}}}(\tau, t)$ to τ.

Calculation of the autocorrelation and spectral density of $\mathcal{T}(t)$ requires some special attention. Each separate term in $\mathcal{T}(t)$, denoted by $\mathcal{T}_n(t)$, equals the product of a noise current $i_n(t)$ and a (noise-free) function of the signal currents, $G_n(t)$. Often $i_n(t)$ is a shot-noise process corresponding to a collector current $I_n(t)$ that is included in $G_n(t)$. In that case, $i_n(t)$ is statistically dependent on $G_n(t)$. The autocorrelation $R_{\mathcal{T}_n}(\tau, t)$ of the term $i_n(t)G_n(t)$ should then be calculated as a conditional expectation over i_n, followed by an expectation over $\vec{s}$

$$\begin{aligned} R_{\mathcal{T}_n}(\tau, t) &= E\{E[i_n(t+\tau)i_n(t)|\vec{s}(t)]_{i_n} G_n(t+\tau)G_n(t)\}_{\vec{s}(t)} \\ &= E\{R_{i_n}[\tau, t|\vec{s}(t)]G_n(t+\tau)G_n(t)\}_{\vec{s}(t)} \end{aligned} \tag{18}$$

where $R_{i_n}[\tau, t, \vec{s}(t)]$ denotes the autocorrelation of i_n, conditioned on the input signals $\vec{s}$. Alternatively, in case of a deterministic "signal," the expectation over $\vec{s}$ can be replaced by a time-average.

For a nonstationary shot-noise process follows that

$$R_{i_n}[\tau, t|\vec{s}(t)] = qI_n(t)\delta(\tau). \tag{19}$$

Then, the power spectral density of $\mathcal{T}_n(t)$ becomes

$$S_{\mathcal{T}_n}(\omega, t) = qE\big[I_n(t)G_n^2(t)\big]_{\vec{s}(t)}. \tag{20}$$

D. Output SNR

The final step is the determination of the circuit's output SNR for a given input signal. For a meaningful interpretation, both the signal power and the noise power in the SNR expression should preferably be independent of time. However, when the input signals $\vec{s}(t)$ are deterministic or nonstationary, the noise power obtained by integration of (20) over ω is time-dependent.

A convenient way to arrive at time-independent SNR is then to average the power, or equivalently the power spectral density, over time.

V. Noise in Static Translinear Circuits

This section applies the proposed noise analysis method to some generic static TL circuits. The most simple example, a current mirror, is analyzed first. Subsequently, two examples of circuits containing a second-order TL loop, a square circuit and a square root circuit, are considered. Finally, a geometric mean current splitter is analyzed. Its noise behavior is very interesting, since the current splitter is used in many TL filters to increase the DR through class AB operation.

A. Current Mirror

The current mirror is the simplest TL circuit. Whereas, in general, TL circuits are described by products of currents, the current mirror is described by a first-order polynomial, which contains no multiplications. Therefore, one of the two previously identified mechanisms of signal–noise intermodulation does not occur in this circuit. The only source of signal–noise intermodulation is thus the transformation of the noise voltage v_{R_B} into a noise current i_{R_B}.

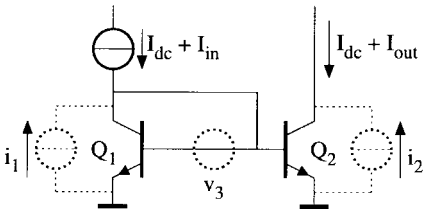

Fig. 6. Relevant noise sources in a current mirror.

Fig. 6 shows a two-transistor current mirror, biased in class A by a dc current $I_{\rm dc}$. The zero-mean input current $I_{\rm in}$ and output current $I_{\rm out}$ are superposed on $I_{\rm dc}$. The three relevant noise sources of the circuit are the shot noise sources i_1 and i_2, and the noise voltage source v_3, representing the total thermal noise of Q_1 and Q_2.

First, the voltage source v_3 has to be transformed into an equivalent noise current source. To this end, multiplication of v_3 by the *time-dependent* transconductance $g_{m_1} = (I_{\rm dc} + I_{\rm in})/U_T$ of Q_1 yields an equivalent noise current source i_3 in parallel with i_1, given by

$$i_3 = (I_{\rm dc} + I_{\rm in})\,\frac{v_3}{U_T}. \tag{21}$$

Clearly, the product $I_{\rm in}v_3$ in (21) represents the signal–noise intermodulation present in i_3.

When all transistor nonidealities are neglected, the input–output relation is easily obtained by rewriting the TL loop equation of the circuit, i.e., $(I_1 + i_1 + i_3) = (I_2 + i_2)$. Rearranging the terms yields

$$I_{\rm out} = I_{\rm in} + i_1 - i_2 + (I_{\rm dc} + I_{\rm in})\,\frac{v_3}{U_T}. \tag{22}$$

The output current $I_{\rm out}$ can be divided into three components by a application of (17a)–(17c). This yields

$$\mathcal{C}(t) = 0 \tag{23a}$$

$$\mathcal{S}(t) = I_{\rm in} \tag{23b}$$

$$\mathcal{T}(t) = i_1 - i_2 + v_3\,\frac{I_{\rm dc} + I_{\rm in}}{U_T}. \tag{23c}$$

Obviously, since multiplications of collector currents are absent, i_1 and i_2 do not introduce any signal–noise intermodulation. Alternatively, this is intuitively clear since i_1 and i_2 are situated at the input and output, respectively, and the overall transfer function of the circuit is linear.

For this circuit, calculation of the autocorrelation and power spectral density of the total output noise $\mathcal{T}(t)$ is relatively simple. All terms are mutually independent, and also the factors v_3 and $I_{\rm dc} + I_{\rm in}$ in the last term are independent. The autocorrelation of $\mathcal{T}(t)$, conditioned on $\vec{s}(t) = I_{\rm in}$ is then found as

$$R_{\mathcal{T}}(\tau, t|I_{\rm in}) = R_{i_1}(\tau, t|I_{\rm in}) + R_{n_2}(\tau, t|I_{\rm in}) + R_{v_3}(\tau)\,\frac{[I_{\rm dc} + I_{\rm in}(t)]^2}{U_T^2} \tag{24}$$

where $R_{i_1}(\tau, t|I_{\rm in})$, $R_{i_2}(\tau, t|I_{\rm in})$, and $R_{v_3}(\tau)$ are the autocorrelation functions of i_1, i_2, and v_3, respectively. Since i_1 and i_2 are shot noise currents, their (conditional) autocorrelation

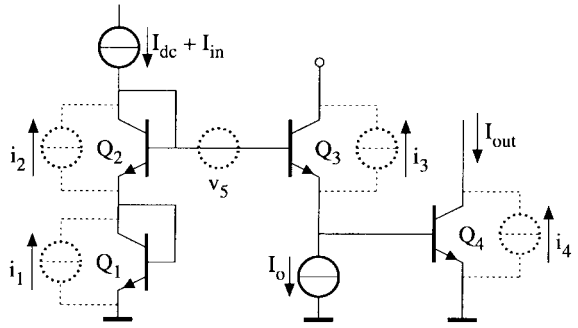

Fig. 7. Translinear square circuit with internal noise sources.

satisfies (19). The corresponding collector signal currents follow from the (noise-free) TL equation

$$I_1 = I_2 = I_{\rm dc} + I_{\rm in}.$$

The power spectral density of $\mathcal{T}(t)$, conditioned on $I_{\rm in}$, follows by Fourier transformation of (24)

$$S_{\mathcal{T}}(\omega, t|I_{\rm in}) = 2q[I_{\rm dc} + I_{\rm in}(t)] + \frac{4kTR_B[I_{\rm dc} + I_{\rm in}(t)]^2}{U_T^2} \tag{25}$$

where the shot-noise autocorrelation (19) is substituted for i_1, i_2. A time-independent spectral density, which is preferable for the output SNR, can be obtained by taking the expectation over a stationary input $I_{\rm in}(t)$. To this end, let $I_{\rm in}$ be a sine wave at frequency ω_o, given by

$$I_{\rm in} = mI_{\rm dc}\,\sin(\omega_o t + \phi) \tag{26}$$

where m is the modulation index with respect to the dc bias current $I_{\rm dc}$, and ϕ is a uniformly distributed stochastic variable, representing the arbitrary choice of the origin of the time axis. Then, the expectation of (25) over ϕ yields

$$S_{\mathcal{T}}(\omega) = 2q\left[I_{\rm dc} + \frac{2R_B(I_{\rm dc}^2 + P_{I_{\rm in}})}{U_T}\right] \tag{27}$$

$$= 2qI_{\rm dc}\left[1 + \frac{2R_BI_{\rm dc}}{U_T}\left(1 + \frac{1}{2}m^2\right)\right]. \tag{28}$$

The term including the input power $P_{I_{\rm in}}$ in (27) would not have been obtained from a standard small-signal noise analysis of the circuit in its quiescent point. From (28) it follows that at high current levels, where R_B dominates the noise, the total output noise can increase up to 1.8 dB (a factor 1.5) for $m = 1$ in case of a sinusoidal input signal. At low current levels, only "linear noise" can be observed.

B. Square Circuit

The square circuit depicted in Fig. 7, which can be applied, e.g., as a frequency doubler, contains a second-order TL loop. The four transistors each contribute a noise source i_1–i_4. The collector currents of Q_1 and Q_2 equals the input signal, superposed on a DC bias current.

The four noise voltage sources are combined into one source v_5. Because transistor Q_3 is biased at a constant current I_o, v_5 can be elegantly transformed to an equivalent noise current source in parallel with i_3, without introducing (extra)

signal–noise intermodulation terms. To simplify the equations, and without loss of generality, v_5 will be assumed negligible. Including i_1–i_4, the TL loop equation reads

$$(I_{\rm dc}+I_{\rm in}+i_1)(I_{\rm dc}+I_{\rm in}+i_2)=(I_o+i_3)(I_{\rm out}+i_4). \quad (29)$$

The input–output relation, including first-order noise, follows by solving (29) for $I_{\rm out}$, and application of a Taylor approximation to i_1–i_4

$$I_{\rm out}=\frac{(i_1+i_2)(I_{\rm dc}+I_{\rm in})}{I_o}+(I_o-i_3)\frac{(I_{\rm dc}+I_{\rm in})^2}{I_o^2}-i_4. \quad (30)$$

Obviously, due to the nonlinear circuit transfer, all sources, except i_4, which is already at the output, cause signal–noise intermodulation. If again the sinusoidal input signal of (26) is adopted, $I_{\rm out}$ can, using (17a)–(17c), be divided into the following components

$$\mathcal{C}(t)=\frac{I_{\rm dc}^2}{I_o}\left(1+\frac{1}{2}m^2\right) \quad (31a)$$

$$\mathcal{S}(t)=\frac{mI_{\rm dc}^2}{2I_o}[4\sin(\omega_o t+\phi)-m\cos(2\omega_o t+2\phi)] \quad (31b)$$

$$\mathcal{T}(t)=(i_1+i_2)\frac{I_{\rm dc}+I_{\rm in}}{I_o}-i_3\frac{(I_{\rm dc}+I_{\rm in})^2}{I_o^2}-i_4. \quad (31c)$$

Equation (31c) reveals that i_1 and i_2 are modulated only by the fundamental frequency, whereas i_3 is also modulated by the second harmonic frequency component. Further, (31a) shows that the DC level of the output transistor is a function of the modulation index m.

The power spectral density of $\mathcal{C}(t)$ and $\mathcal{S}(t)$ follows straightforward from (31a) and (31b). For the spectral density of $\mathcal{T}(t)$, conditioned on $\vec{s}=I_{\rm in}$, we obtain

$$S_{\mathcal{T}}(\omega,t|I_{\rm in})=\frac{q(I_{\rm dc}+I_{\rm in})^2}{I_o}+\frac{2q(I_{\rm dc}+I_{\rm in})^3}{I_o^2}+\frac{q(I_{\rm dc}+I_{\rm in})^4}{I_o^3}. \quad (32)$$

By taking the expectation over ϕ, the stochastic variable in $I_{\rm in}$, the following time-independent power spectral density is obtained

$$S_{\mathcal{T}}(\omega)=\frac{qI_{\rm dc}^2}{I_o}\left[\left(1+\frac{1}{2}m^2\right)+\frac{I_{\rm dc}}{I_o}(2+3m^2)+\frac{I_{\rm dc}^2}{8I_o^2}(8+24m^2+3m^4)\right]. \quad (33)$$

Suppose that an equivalent noise bandwidth $2B$ around $2\omega_o$ is of interest. The SNR in this band, obtained from (31b) and integration of (33), equals (34), shown at the bottom of the page. For large values of $I_{\rm dc}$, this SNR approaches

$$\lim_{I_{\rm dc}\to\infty}\ {\rm SNR}=\frac{I_o}{2Bq}\frac{m^4}{3m^4+24m^2+8}, \quad (35)$$

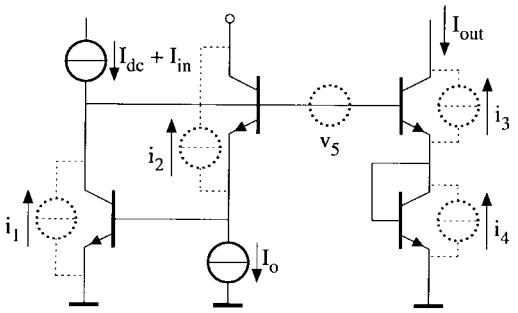

Fig. 8. Translinear square-root circuit in the presence of noise.

which, according to (10) for $R_B=0$, is always smaller than the SNR of Q_3. The latter conclusion shouldn't be a surprise. As $I_{\rm dc}$ increases, the power contents of the collector currents through all transistors, in the loop, except Q_3, increases. Consequently, also their SNR increases. Since a TL loop is basically a cascade of transistors, Q_3 will finally limit the SNR in the entire loop.

A major advantage of symbolic expressions for the SNR the possibility to perform optimizations. As an example, consider the relation between I_o and $I_{\rm dc}$, which can be optimized for a given input signal. If $m=1/2$, it follows from the derivative of (34) with respect to I_o that $I_o=I_{\rm dc}\sqrt{227}/12$ maximizes the SNR.

C. Square-Root Circuit

Another example of a second-order TL loop is found in the square-root circuit of Fig. 8.

The input–output relation for this circuit, including first-order noise, equals

$$I_{\rm out}=\sqrt{(I_{\rm dc}+I_{\rm in})I_o}+\frac{1}{2}\left(i_1\sqrt{\frac{I_o}{I_{\rm dc}+I_{\rm in}}}+i_2\sqrt{\frac{I_{\rm dc}+I_{\rm in}}{I_o}}-i_3-i_4\right). \quad (36)$$

In this case, it is not possible, or at least very cumbersome, to find an analytical expression for $\mathcal{C}$. However, it is directly clear from (36) that the first term on the RHS equals $\mathcal{C}+\mathcal{S}$ and the second term represents the total noise $\mathcal{T}$. Using the proposed analysis method, the spectrum of $\mathcal{T}$ conditioned on $I_{\rm in}$ is found to be

$$S_{\mathcal{T}}(\omega,t|I_{\rm in})=\frac{q}{4}\left[I_o+I_{\rm dc}+I_{\rm in}+2\sqrt{(I_{\rm dc}+I_{\rm in})I_o}\right]. \quad (37)$$

Again, a time-independent spectrum is obtained by taking the expectation over $I_{\rm in}$. For the sinusoidal input signal from (26), the expectation of the square-root in (37) equals approximately $\sqrt{I_oI_{\rm dc}}(1-\frac{1}{16}m^2)$. Thus, $S_{\mathcal{T}}(\omega)$ becomes

$$S_{\mathcal{T}}(\omega)=\frac{q}{4}\left[I_o+I_{\rm dc}+2\sqrt{I_oI_{\rm dc}}\left(1-\frac{1}{16}m^2\right)\right]. \quad (38)$$

$$\text{SNR}=\frac{I_o}{2Bq}\frac{I_{\rm dc}^2m^4}{I_{\rm dc}^2(3m^4+24m^2+8)+8I_{\rm dc}I_o(3m^2+2)+4I_o^2(m^2+2)} \quad (34)$$

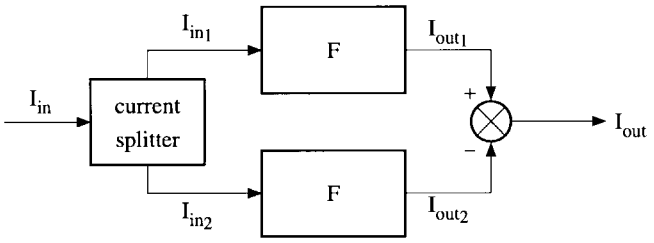

Fig. 9. Principle of class AB operation.

D. Class AB Current Splitters

The current flowing through a transistor is always restricted to positive values. To facilitate the processing of signals of both negative and positive polarity, some kind of biasing is required. One possible solution is class A operation, where the actual signal is superposed on a dc bias current. The maximal negative current signal swing is now limited to the dc value of the bias current.

Another option is class B or class AB operation. A well-known example is the push–pull output stage used in many opamps. In class (A)B, an input signal $I_{\rm in}$ is split up into two strictly positive signals $I_{\rm in_1}$ and $I_{\rm in_2}$. The difference of these signals equals the original signal $I_{\rm in}$. Although $I_{\rm in_1}$ and $I_{\rm in_2}$ are strictly positive, the difference $I_{\rm in_1} - I_{\rm in_2}$ can take on negative values, thus facilitating processing of bipolar signals. The two signals $I_{\rm in_1}$ and $I_{\rm in_2}$ are processed by separate paths, as illustrated in Fig. 9. These signal paths can consist of complete TL filters, as proposed in [42]. But, it is also possible to apply class AB operation within a TL filter. As an example, we mention the class of $\sinh$ filters [16], [33], [43]. Class AB operation is not restricted to dynamic TL circuits. It can also be applied, e.g., in four-quadrant multipliers.

The input current has to be split into two separate signal paths. In the equation $I_{\rm in} = I_{\rm in_1} - I_{\rm in_2}$, two new variables are introduced. Consequently, an additional expression is required to fix the relation between $I_{\rm in_1}$ and $I_{\rm in_2}$. In class B, $I_{\rm in_1}$ equals $I_{\rm in}$ when $I_{\rm in} > 0$ and zero otherwise. When $I_{\rm in}$ is negative, $I_{\rm in_2} = -I_{\rm in}$, and zero otherwise. An important disadvantage of class B operation is cross-over distortion. Class AB operation eliminates this disadvantage. In a class AB circuit, the transistors are never completely turned off. Here, another equation is chosen to establish the relation between $I_{\rm in_1}$ and $I_{\rm in_2}$. Often, the geometric mean function is used, which can be implemented by the circuit shown in Fig. 10. Thus, $I_{\rm in_1}$ and $I_{\rm in_2}$ are described by

$$I_{\rm in_{1,2}} = \frac{1}{2}\left(\sqrt{4I_{dc}^2 + I_{\rm in}^2} \pm I_{\rm in}\right). \tag{39}$$

Another possibility is the harmonic mean. This function has the advantage that $I_{\rm in_1}$ and $I_{\rm in_2}$ always remain larger than $I_{\rm dc}$. Thus, the transit frequencies of the transistors of the splitter maintain a certain minimum value [44].

As class AB operation can increase the DR of a TL filter, the noise behavior of the current splitter shown in Fig. 10 is very relevant.

The output current of the splitter equals the difference of $I_{\rm in_1}$ and $I_{\rm in_2}$. Looking at the node at which the input current source is connected, it is clear that the output current equals $I_{\rm in}$, irrespective of the noise sources. This means that the splitter itself does not add any noise. The noise sources present in the TL loop equation of the geometric mean circuit only result in common-mode noise in $I_{\rm in_1}$ and $I_{\rm in_2}$, which is irrelevant. In many circuit implementations, additional current mirrors are used in order to supply $I_{\rm in_1}$ and $I_{\rm in_2}$ to the subsequent signal paths. The noise contribution of these current mirrors can be decreased using emitter degeneration resistors.

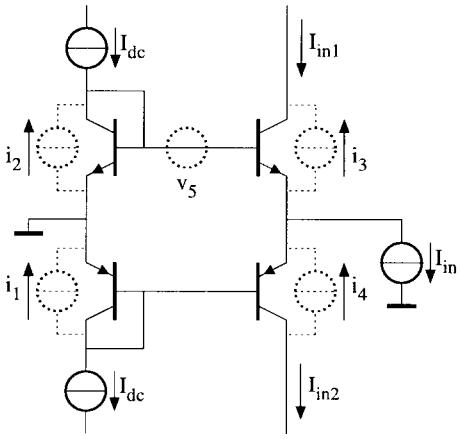

Fig. 10. Geometric mean current splitter in the presence of noise.

VI. Noise in Dynamic Translinear Circuits

In this section, the nonlinear noise properties of TL filters are examined. Although the proposed nonlinear noise analysis method is, in principle, applicable both to linear and nonlinear dynamic TL circuits, the analyzes presented in this section are limited to linear filters. A kind of exception is formed by the class AB filter introduced by Seevinck in [2], which is described by a system of nonlinear DE's.

First, a first-order class A filter and the corresponding class AB filter are examined. Subsequently, Seevinck's class AB filter circuit is treated.

A. Class-A Translinear Filter

Fig. 11 shows a well-known first-order DTL low-pass filter, operated in class A. It consists of a second-order TL loop, comprising Q_1–Q_4, and a capacitance C. The cut-off frequency can be tuned by the current I_o.

The first, the noise voltages v_5 and v_6, representing the thermal noise of Q_1–Q_2 and Q_3–Q_4, respectively, have to be transformed into an equivalent noise current. Due to the presence of C in the TL loop, v_5 and v_6 cannot be combined into a single equivalent noise voltage, but have to be transformed into separate noise currents i_5 and i_6 in parallel with i_1 and i_4. This yields the TL equation [26]

$$\begin{aligned}&(I_{\rm dc} + I_{\rm in} + i_1 + i_5)(I_o + i_3)\\ &\quad = (I_o + I_{\rm cap} + i_2)(I_{\rm dc} + I_{\rm out} + i_4 + i_6).\end{aligned} \tag{40}$$

The capacitance current $I_{\rm cap}$ can be eliminated using (3). After Taylor approximation, this yields for the input–output relation,

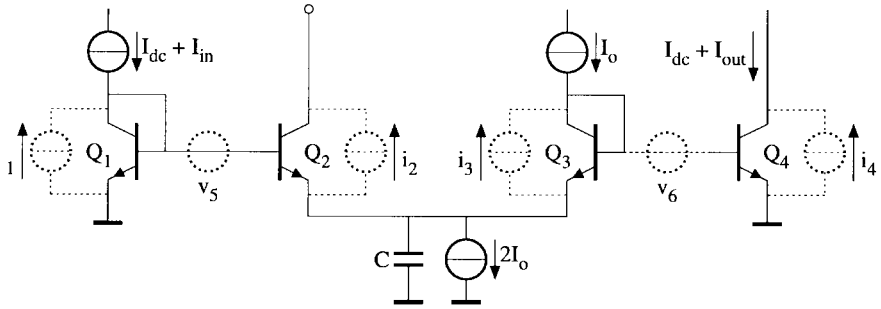

Fig. 11. Noise in a translinear first-order low-pass filter.

including first-order noise

$$\frac{CU_T}{I_o}\left[\dot{I}_{\text{out}}+\frac{d}{dt}(-i_{3,eq}+i_4+i_6)\right]+I_{\text{out}}-i_{3,eq}+i_4+i_6 = I_{\text{in}}+i_1+i_5-i_2\,\frac{I_{\text{dc}}+I_{\text{out}}}{I_o} \tag{41}$$

where $i_{3,eq}=i_3\cdot(I_{\text{dc}}+I_{\text{out}})/I_o$. This equation shows that i_1, i_2, and i_5 are situated at the input, whereas $i_{3,eq}$, i_4, and i_6 are located at the filter output. Hence, two (conditional) noise spectra $S_{\mathcal{I}_{\text{in}}}(\omega,\, t|I_{\text{in}})$ and $S_{\mathcal{I}_{\text{out}}}(\omega,\, t|I_{\text{in}})$ can be distinguished

$$S_{\mathcal{I}_{\text{in}}}(\omega,\, t|I_{\text{in}}) = q\left[\underbrace{I_{\text{dc}}+I_{\text{in}}}_{i_1}+\underbrace{\frac{(I_o+I_{\text{cap}})(I_{\text{dc}}+I_{\text{out}})^2}{I_o^2}}_{i_2}+\underbrace{\frac{4R_B(I_{\text{dc}}+I_{\text{in}})^2}{U_T}}_{v_5}\right] \tag{42a}$$

$$S_{\mathcal{I}_{\text{out}}}(\omega,\, t|I_{\text{in}}) = q\left[\underbrace{\frac{(I_{\text{dc}}+I_{\text{out}})^2}{I_o}}_{i_3}+\underbrace{I_{\text{dc}}+I_{\text{out}}}_{i_4}+\underbrace{\frac{4R_B(I_{\text{dc}}+I_{\text{out}})^2}{U_T}}_{v_6}\right]. \tag{42b}$$

The horizontal braces indicate the origin of the different terms.

Subsequently, the spectrum $S_{\mathcal{I}_{\text{in}}}(\omega,\, t)$ has to be transformed to the output. In principle, transformation of a time-dependent spectrum requires two-dimensional Fourier transforms. However, since the overall filter transfer $H(j\omega)$ is linear time-invariant, the order of transformation of $S_{\mathcal{I}_{\text{in}}}$ and the expectation over I_{in} can be exchanged. In this way, the Wiener–Kintchine theorem can be used to transform $S_{\mathcal{I}_{\text{in}}}(\omega)$ to the output. Substitution of (3) and using that $E[I_{\text{out}}(d/dt)I_{\text{out}}]=0$ [45], the time-independent output noise spectrum becomes

$$S_{\mathcal{I}}(\omega)=\frac{4qR_B}{U_T}\left[P_{I_{\text{out}}}+P_{I_{\text{in}}}|H(j\omega)|^2\right]+q\left(I_{\text{dc}}+\frac{I_{\text{dc}}^2+P_{I_{\text{out}}}}{I_o}+\frac{4R_BI_{\text{dc}}^2}{U_T}\right)\cdot\left[1+|H(j\omega)|^2\right]. \tag{43}$$

Equation (43) shows that intermodulation of the noise sources with both the input and the output signal occurs, even when the input signal is located outside the pass-band of the filter. Consequently, a large out-of-band-signal will deteriorate the SNR of a small in-band-signal at the output of the filter. Though, the intermodulation noise is higher for in-band signals as for out-of-band signals.

Since $m<1$ for a class-A filter, the influence of signal $\times$ noise intermodulation is very small. The difference between the nonlinear calculation and the linear approximation for this filter equals only 1.51 dB for $m=1$ (maximum signal current equal to bias current). Hence, for class-A TL filters, the noise floor in the absence of any signals can be used as a good estimate of the noise. This is not the case in class-AB filters, as is shown next.

B. Class-AB Translinear Filter

Class-AB operation can be used to benefit from the DR improvement provided by companding. A first-order class-AB filter can, according to Fig. 9, be constructed from two filters of the type depicted in Fig. 11. Since the input currents I_{in_1} and I_{in_2} of both filters in such a configuration are strictly positive, the DC bias current I_{dc} becomes obsolete and is omitted. The output currents are denoted by I_{out_1} and I_{out_2}. The SNR of the resulting class-AB filter is calculated for the sine wave input I_{in} of (26).

As shown in Section V, the current splitter does not contribute any noise. Assuming the current mirrors between the splitter and two class-A filters do not have a significant noise contribution, the equivalent output noise power equals two times the equivalent output noise power of one class-A filter. Neglecting the influence of R_B, the output noise spectrum $S_{\mathcal{I},\mathcal{I}_{\text{in}_1}}(\omega)$ of one class-A filter equals

$$S_{\mathcal{I},\mathcal{I}_{\text{in}_1}}(\omega)=q\left(\frac{P_{I_{\text{out}_1}}}{I_o}+\overline{I_{\text{out}_1}}\right)\left[1+|H(j\omega)|^2\right] \tag{44}$$

where $\overline{I_{\text{out}_1}}\,(=\overline{I_{\text{in}_1}})$ is the DC average value of I_{out_1}, $P_{I_{\text{out}_1}}$ is the power of I_{out_1} and $H(j\omega)$ is the transfer function of the filter.

The noise floor in class-AB filters increases due to two effects. Signal $\times$ noise intermodulation saturates the SNR, while an increase of $\overline{I_{\text{out}_1}}$, having a much weaker effect, increases the noise without causing saturation.

The output SNR for an input signal located in the pass band can be determined as follows. For such a signal, the

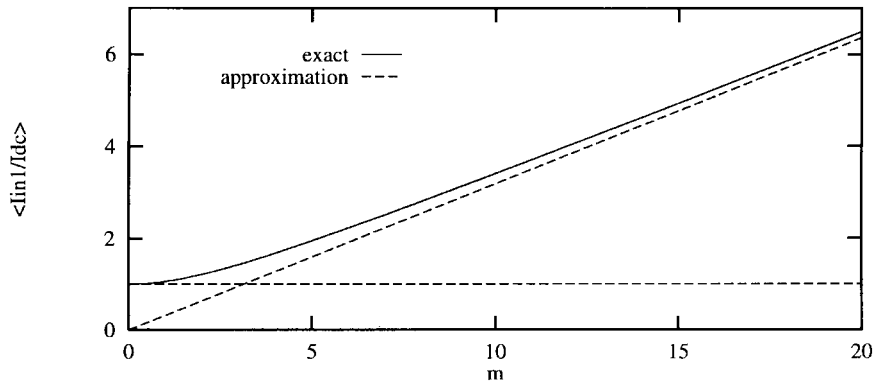

Fig. 12. DC output level of a geometric mean splitter.

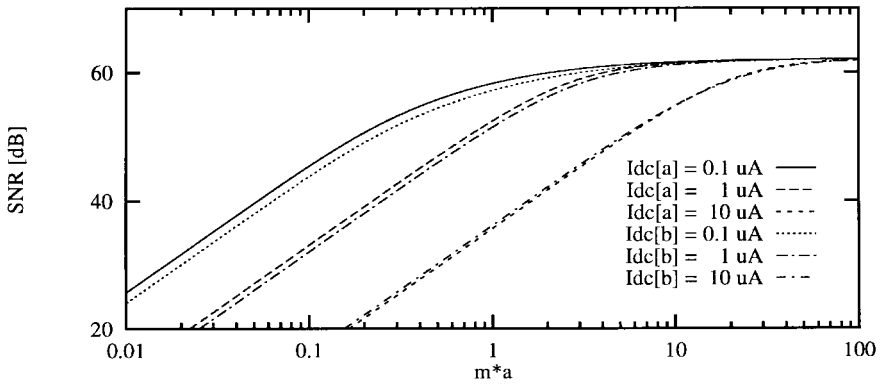

Fig. 13. Signal-to-noise-ratio of a class-AB translinear filter. $I_{\rm dc}[a]$: filter based on Fig. 11. $I_{\rm dc}[b]$: filter of Fig. 14.

filter transfer amounts to unity, such that $P_{I_{\rm out_1}} \approx P_{I_{\rm in_1}}$. Application of a geometric current splitter then yields

$$P_{I_{\rm in_1}} = \overline{I_{\rm in_1}^2} = I_{\rm dc}^2\left(1 + \tfrac{1}{4}m^2\right). \tag{45}$$

An exact expression for the average value $\overline{I_{\rm in_1}}$ for the sine wave input, see (26), cannot be computed. However, $\overline{I_{\rm in_1}}$ can be approximated by

$$\overline{I_{\rm in_1}} = \begin{cases} I_{\rm dc}, & \text{if } m \ll 1 \\ \dfrac{mI_{\rm dc}}{\pi}, & \text{if } m \gg 1. \end{cases} \tag{46}$$

The exact value of $\overline{I_{\rm in_1}}$ and the approximations, (46), are illustrated in Fig. 12.

The total output noise power of the class-AB filter equals twice the value found by integration of (44) over ω. The (double-sided) noise bandwidth of the filter, equal to $I_o/(2CU_T)$, also applied to i_3 and i_4, shown in Fig. 11. For large values of m, the SNR is then given by

$$\text{SNR} = \frac{\frac{1}{2}m^2 I_{\rm dc}^2}{\dfrac{2qI_{\rm dc}}{CU_T}\left[\dfrac{mI_o}{\pi} + I_{\rm dc}\left(1 + \dfrac{1}{4}m^2\right)\right]}. \tag{47}$$

Fig. 13 displays the SNR as a function of m, using the exact value of $\overline{I_{\rm in_1}}$. For the parameter $a = I_{\rm dc}/I_o$ the values $a = [0.1, 1, 10]$ are used. Further, I_o = 1 μA, $C = 10$ pF, and $U_T = 26$ mV. The corresponding cut-off frequency is 612 kHz. Thus, the x-axis variable $m \cdot a$, represents the amplitude of $I_{\rm in}$, normalized to I_o. For low values of $m \cdot a$, the SNR increases linearly, by 20 dB per decade. Eventually, it saturates to a value of 62.1 dB.

As illustrated by Fig. 13, a higher value of $I_{\rm dc} = I_{\rm dc}[a]$ yields a higher noise floor and a lower SNR. A lower value of $I_{\rm dc}$ decreases the output noise, but also increases the distortion at a certain input power level. These two effects will have to be mutually weighed during design.

As follows from (47) the maximal SNR equals

$$\lim_{m\to\infty} \text{SNR} = \frac{CU_T}{q}. \tag{48}$$

This results leads to the interesting conclusion that the maximal SNR not only increases linearly with the capacitance C, but also with the absolute temperature T. This effect can be explained as follows. On one hand, the shot noise is independent of the temperature. On the other hand, according to (3), the capacitance voltage (and current) swings increase proportional to T, which is beneficial with respect to the SNR. Except for a constant factor, (48) complies with (10), when $R_B = 0$, $I_C = I_o$ (the lowest collector current in the class-AB filter), and $B = I_o/2CU_T$. For high current levels, where the base resistance noise dominates, the same conclusion is reached. In this region, the maximal SNR equals

$$\lim_{m\to\infty} \text{SNR} = \frac{CU_T}{q}\,\frac{U_T}{4R_B I_o}. \tag{49}$$

The first fraction on the RHS corresponds with (48). The second fraction is temperature independent, since I_o has to

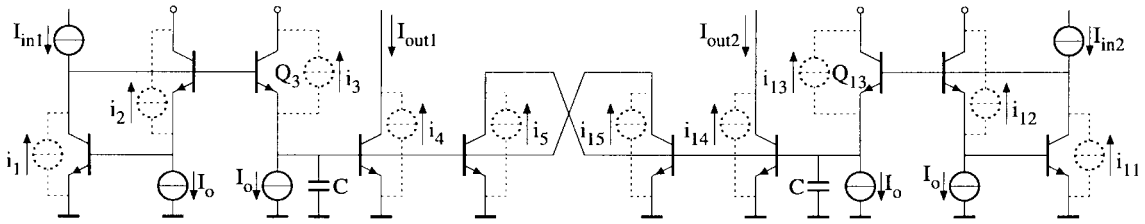

Fig. 14. Noise in Seevinck's class-AB translinear filter [2].

be a PTAT current to prevent a temperature dependent cut-off frequency [1], [2].

Consider $m = 15$ as an estimate for the practical upper limit of the signal swing. For this modulation index, and $a = [0.1, 1, 10]$, the filter DR equals $[79.2, 86.6, 89.2]$ dB, respectively. The differences of $[17.1, 24.5, 27.1]$ dB, respectively, between the DR and the SNR demonstrates the beneficial influence of companding.

C. Seevinck's Class-AB Integrator

Although exhibiting an externally-linear transfer function, the class-AB integrator proposed by Seevinck in [2], shown in Fig. 14, is in a way a nonlinear DTL circuit. It implements two nonlinear DE's

$$CU_T\dot{I}_{\text{out}_{1,2}} + I_o I_{\text{out}_{1,2}} + I_{\text{out}_1} I_{\text{out}_2} = I_o I_{\text{in}_{1,2}}. \tag{50}$$

Two current sources I_o are added in parallel to the capacitances to give the circuit the same transfer from $I_{\text{in}_1} - I_{\text{in}_2}$ to $I_{\text{out}_1} - I_{\text{out}_2}$ as the filter shown in Fig. 11.

The most important change with respect to the class-AB filter treated previously is the addition of the output currents I_{out_1} and I_{out_2} to the collector currents of Q_{13} and Q_3, respectively. This assures all collector currents to be strictly positive when the circuit is used as an integrator.

The circuit basically comprises two TL loops, the inputs I_{in_1} and I_{in_2} of which are obtained from a (geometric mean) current splitter. The difference of I_{out_1} and I_{out_2} is the actual output current I_{out}. The input–output relation, including first-order noise

$$\begin{aligned}\frac{CU_T}{I_o}\left(\dot{I}_{\text{out}} + \frac{di_4}{dt} - \frac{di_{14}}{dt}\right) + I_{\text{out}} + i_4 - i_{14} \\ = I_{\text{in}} + i_1 - i_{11} + i_2\frac{I_{\text{in}_1}}{I_o} - i_{12}\frac{I_{\text{in}_2}}{I_o} + (i_{15} - i_3)\frac{I_{\text{out}_1}}{I_o} \\ + (i_{13} - i_5)\frac{I_{\text{out}_2}}{I_o}.\end{aligned} \tag{51}$$

Calculation of $S_{\mathcal{T}}$ is complicated by i_4 and i_{14}, since these sources contribute to both the filter input and output. In this case, the easiest solution is obtained by moving all terms with i_4, i_{14} to the RHS, i.e., to the filter input. Since i_4 and i_{14} are white, it can be shown that they are uncorrelated with their time derivatives for all time-differences τ. Using this observation, it follows that the contribution of i_4 to $S_{\mathcal{T}}$ equals $qE[I_{\text{out}_1}] + (q/I_o^2)|H(j\omega)|^2 E[I_{\text{out}_2}^2 I_{\text{out}_1} + 2I_o I_{\text{out}_1} I_{\text{out}_2}]_{I_{\text{in}}}$. Using (50) to substitute for $I_{\text{out}_1} I_{\text{out}_2}$ in the expectations and assuming a symmetrical input signal, we finally arrive at

$$\begin{aligned}S_{\mathcal{T}}(\omega) = 2qE[I_{\text{out}_1}]_{I_{\text{in}}} + \frac{2q}{I_o}\left(P_{I_{\text{in}_1}} - 2P_{I_{\text{out}_1}}\right)|H(j\omega)|^2 \\ + 2q|H(j\omega)|^2 \cdot E\left[3I_{\text{in}_1} - 2I_{\text{out}_1} + \frac{3I_{\text{in}_1} I_{\text{out}_1}}{I_o}\right]_{I_{\text{in}}}.\end{aligned} \tag{52}$$

Due to its dependence on I_{out_1}, evaluation of (52) requires the solution of the nonlinear DE's (50). Unfortunately, since there is no general way of doing so, one has to resort to numerical approximation, using a circuit simulator, to find P_{out_1}, $E[I_{\text{out}_1}]$ and $E[I_{\text{in}_1} I_{\text{out}_1}]$.

The output SNR for this filter is depicted in Fig. 13 as a function of $I_{\text{dc}} = I_{\text{dc}}[b]$, using the same parameter values that were used to generate the curves for $I_{\text{dc}}[a]$. For low ratios $a = I_{\text{dc}}/I_o$, the SNR of the filter of Fig. 14 is slightly lower than the SNR of the other class-AB filter, while for high ratios it is higher better.

VII. Conclusions

Due to their explicit dependence on the exponential characteristic of the transistor, static and dynamic translinear circuits exhibit a strongly nonlinear noise behavior, even when the overall current-mode transfer is linear.

To fully appreciate TL technology, noise analysis is of fundamental importance. However, due to the presence of signal–noise intermodulation and nonstationary noise, such analysis cannot be accomplished through standard small-signal techniques. Instead, a more advanced approach, based on the large-signal equations, has to be developed. This is not a trivial task. Most circuit simulators also do not provide such a nonlinear noise analysis.

This paper presents a method to determine the first-order nonlinear output noise and signal–noise intermodulation of static and dynamic TL circuits, using the existing current-mode analysis methods for these circuits. On the hand of some generic static and dynamic examples, it is shown how to calculate the maximal SNR, an important filter specification. Further, it is shown that the maximal SNR of each TL loop in a TL circuit is fundamentally limited to the SNR of the transistor biased at the lowest current. As shown, this finally causes saturation of the output SNR in class-AB filters for increasing input power.

References

[1] R. W. Adams, "Filtering in the log domain," in *63rd Conv. AES*, May 1979, preprint 1970.

[2] E. Seevinck, "Companding current-mode integrator: A new circuit principle for continuous-time monolithic filters," *Electron. Lett.*, vol. 26, no. 24, pp. 2046–2047, Nov. 1990.

[3] D. R. Frey, "Log-domain filtering: An approach to current-mode filtering," *Proc. Inst. Elect. Eng. G*, vol. 140, no. 6, pp. 406–416, Dec. 1993.
[4] C. Toumazou, J. Ngarmnil, and T. S. Lande, "Micropower log-domain filter for electronic cochlea," *Electron. Lett.*, vol. 30, no. 22, pp. 1839–1841, Oct. 1994.
[5] D. Perry and G. W. Roberts, "Log-domain filters based on LC ladder synthesis," in *Proc. ISCAS*, 1995, vol. 1, pp. 311–314.
[6] M. Punzenberger and C. Enz, "Low-voltage companding current-mode integrators," in *Proc. ISCAS*, 1995, vol. 3, pp. 2112–2115.
[7] W. A. Serdijn, M. Broest, J. Mulder, A. C. van der Woerd, and A. H. M. van Roermund, "A low-voltage ultra-low-power current-companding integrator for audio filter applications," in *Proc. ESSCIRC*, 1996, pp. 412–415.
[8] J. Mulder, A. C. van der Woerd, W. A. Serdijn, and A. H. M. Van Roermund, "An RMS-DC converter based on the dynamical translinear principle," in *Proc. ESSCIRC*, 1996, pp. 312–315.
[9] B. Gilbert, "Translinear circuits: A proposed classification," *Electron. Lett.*, vol. 11, no. 1, pp. 14–16, Jan. 1975.
[10] S. Pookaiyaudom and J. Mahattanakul, "A 3.3 volt high frequency capacitorless electronically-tunable log-domain oscillator," in *Proc. ISCAS*, 1995, vol. 2, pp. 829–832.
[11] W. A. Serdijn, J. Mulder, A. C. van der Woerd, and A. H. M. van Roermund, "Design of wide-tunable translinear second-order oscillators," in *Proc. ISCAS*, 1997, vol. 2, pp. 829–832.
[12] D. R. Frey and L. Steigerwald, "An adaptive analog notch filter using log filtering," in *Proc. ISCAS*, 1996, vol. 1, pp. 297–300.
[13] A. Thanachayanont, A. Payne, and S. Pookaiyaudom, "A current-mode phase-locked loop using a log-domain oscillator," in *Proc. ISCAS*, 1997, vol. 1, pp. 277–280.
[14] W. A. Serdijn, J. Mulder, and A. H. M. van Roermund, "Dynamic translinear circuits," in *Proc. Workshop on Advances in Analog Circuit Design*, 1998.
[15] D. R. Frey, "Explicit log domain root-mean-square detector," U.S. Patent 5 585 757, Dec. 1996.
[16] W. A. Serdijn, M. H. L. Kouwenhoven, J. Mulder, A. C. van de Woerd, and A. H. M. van Roermund, "Design of high dynamic range fully integratable translinear filters," *Analog Integr. Circuits Signal Process.*, vol. 11, 1998.
[17] D. Frey, "Log domain filtering for RF applications," *IEEE J. Solid-State Circuits*, vol. 31, pp. 1468–1475, Oct. 1996.
[18] Y. Tsividis, "Externally linear, time-invariant systems and their application to companding signal processors," *IEEE Trans. Circuits Syst. II*, vol. 44, pp. 65–85, Feb. 1997.
[19] M. Punzenberger and C. C. Enz, "A 1.2V BiCMOS class AB log-domain filter," in *Proc. ISSCC*, 1997, pp. 56–57.
[20] ———, "Noise in instantaneous companding filters," in *Proc. ISCAS*, 1997, vol. 1, pp. 337–340.
[21] J. Mulder, M. H. L. Kouwenhoven, and A. H. M. van Roermund, "Signal–noise intermodulation in translinear filters," *Electron. Lett.*, vol. 33, no. 14, pp. 1205–1207, July 1997.
[22] C. C. Enz, "Low-power log-domain continuous-time filters: An introduction," in *Low Power—Low Voltage Workshop at ESSCIRC'95*, 1995.
[23] F. Yang, C. Enz, and G. van Ruymbeke, "Design of low-power and low-voltage log-domain filters," in *Proc. ISCAS*, 1996, vol. 1, pp. 117–120.
[24] Y. Z. Bahnas, G. G. Bloodworth, and A. Brunnschweiler, "The noise properties of the linearized transconductance multiplier," *IEEE J. Solid-State Circuits*, vol. 12, no. 5, pp. 580–584, Oct. 1977.
[25] E. Seevinck, *Analysis and Synthesis of Translinear Integrated Circuits*. Amsterdam, The Netherlands: Elsevier, 1988.
[26] J. Mulder, A. C. van der Woerd, W. A. Serdijn, and A. H. M. van Roermund, "General current-mode analysis method for translinear filters," *IEEE Trans. Circuits Syst. I*, vol. 44, pp. 193–197, Mar. 1997.
[27] B. Gilbert, "Translinear circuits: An historical overview," *Analog Integrated Circuits and Signal Processing*, vol. 9, no. 2, pp. 95–118, Mar. 1996.
[28] A. C. van der Woerd, J. Mulder, W. A. Serdijn, and A. H. M. van Roermund, "Recent trends in translinear circuits," in *Proc. Electronics—ET'96*, Sozopol, Bulgaria, 1996, vol. 1, pp. 14–21.
[29] J. Mulder, W. A. Serdijn, A. C. van der Woerd, and A. H. M. van Roermund, "Analysis and synthesis of dynamic translinear circuits," in *Proc. ECCTD*, 1997, vol. 1, pp. 18–23.
[30] J. Mulder, A. C. van der Woerd, W. A. Serdijn, and A. H. M. van Roermund, "Current-mode companding $\sqrt{x}$-domain integrator," *Electron. Lett.*, vol. 32, no. 3, pp. 198–199, Feb. 1996.
[31] M. Eskiyerli, A. Payne, and C. Toumazou, "Square-root domain circuits," in *High Frequency Log & Square-Root Domain Analog Circuits: From Companding to State-Space*, C. Toumazou, A. Payne, and S. Pookaiyaudom, Eds. Oxford, U.K.: Parchment, 1996, Tutorial ICECS'96, Ch. 7, Rados, Greece.
[32] B. Gilbert, "A new wide-band amplifier technique," *IEEE J. Solid-State Circuits*, vol. SC-3, pp. 353–365, Dec. 1968.
[33] D. R. Frey, "Exponential state space filters: A generic current mode design strategy," *IEEE Trans. Circuits Syst. I*, vol. 43, pp. 34–42, Jan. 1996.
[34] M. B. Das, "On the current dependence of low-frequency noise in bipolar transistors," *IEEE Trans. Electron. Devices*, vol. 22, pp. 1092–1098, Dec. 1975.
[35] M. Stegherr, "Arbeitspunktabhängigkeit des $1/f$-rausches integrierter MOS-transistoren," Ph.D. dissertation, Technical Univ. München, Germany, 1984, in German.
[36] E. Vittoz and J. Fellrath, "CMOS analog integrated circuits based on weak inversion operation," *IEEE J. Solid-State Circuits*, vol. SC-12, pp. 224–231, Mar. 1977.
[37] Y. P. Tsividis, *Operation and Modeling of the MOS Transistor*. New York: McGraw-Hill, 1987.
[38] C. C. Enz, F. Krummenacher, and E. A. Vittoz, "An analytical MOS transistor model valid in all regions of operation and dedicated to low-voltage and low-current applications," *Analog Integr. Circuits Signal Process.*, vol. 8, pp. 83–114, July 1995.
[39] J. Fellrath, "Shot noise behavior of subthreshold MOS transistors," *Rev. Phys. Appl.*, no. 13, pp. 719–723, Dec. 1978.
[40] M. H. L. Kouwenhoven, J. Mulder, and A. H. M. van Roermund, "Noise analysis of dynamically nonlinear translinear circuits," *Electron. Lett.*, vol. 34, no. 8, pp. 705–706, Apr. 1998.
[41] N. M. Blachman, "The signal–signal, noise–noise, and signal–noise output of a nonlinearity," *IEEE Trans. Inform. Theory*, vol. IT-14, pp. 21–27, Jan. 1968.
[42] D. Frey, "Current mode class AB second order filter," *Electron. Lett.*, vol. 30, no. 3, pp. 205–206, Feb. 1994.
[43] J. Mahattanakul, C. Toumazou, and A. A. Akbar, "DC stable CCII-based instantaneous companding integrator," in *Proc. ISCAS*, 1997, vol. 2, pp. 821–824.
[44] E. Seevinck, W. de Jager, and P. Buitendijk, "A low-distortion output stage with improved stability for monolithic power amplifiers," *IEEE J. Solid-State Circuits*, vol. 23, pp. 794–801, June 1988.
[45] A. Papoulis, *Probability, Random Variables, and Stochastic Processes*, 3rd ed. New York: McGraw-Hill, 1991.

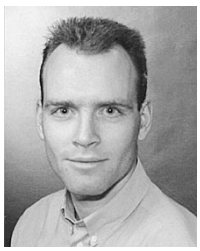

Jan Mulder was born in Medemblik, The Netherlands, on July 7, 1971. He received the M.Sc. degree in electrical engineering from the Delft University of Technology (DUT), Delft, The Netherlands, in 1994. Since 1994, he has been pursuing the Ph.D. degree on static and dynamic-translinear analog integrated circuits at the Electronics Research Laboratory, DUT.

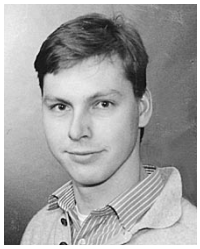

Michiel H. L. Kouwenhoven (S'94–M'98) was born in Delft, The Netherlands, on July 8, 1971. He received the M.Sc. degree in electrical engineering from the Delft University of Technology (DUT) in 1993 and the Ph.D. degree from DUT in 1998 (both *cum laude*).

Since 1997, he has been an Assistant Professor at the Electronics Research Laboratory, DUT, where he is engaged in courses on structured electronic design, a multidisciplinary Ubiquitous Communications (UbiCom) Research Program, and a research program on nonlinear electronics. His main research interests include noise in nonlinear circuits and systems, and the development of design methodologies for wireless communication receivers and demodulators.

Dr. Kouwenhoven received the 1997 Veder Award from the Dutch Foundation for Radio Science for his Ph.D. work on FM demodulators.

Wouter A. Serdijn (M'99) was born in Zoetermeer, The Netherlands, in 1966. He started his course work at the Faculty of Electrical Engineering, Delft University of Technology (DUT), Delft, The Netherlands, in 1984, and received the "Ingenieurs" (M.Sc.) degree in 1989. Subsequently, he joined the Electronics Research Laboratory, DUT, where he received the Ph.D. degree in 1994.

Since 1997, he has been a Project Leader in the multidisciplinary Ubiquitous Communications (UbiCom) Research Program, DUT. His research interests include low-voltage, ultra-low-power, RF and dynamic-translinear analog integrated circuits along with circuits for wireless communications, hearing instruments, and pacemakers. He is coeditor and coauthor of the book *Analog IC Techniques for Low-Voltage Low-Power Electronics* (Delft, The Netherlands: Delft University Press, 1995), and *Low-Voltage Low-Power Analog Integrated Circuits* (Boston, MA: Kluwer, 1995). He authored and coauthored more than 40 publications and presentations. He teaches analog electronics for industrial designers, analog IC techniques, and electronic design techniques.

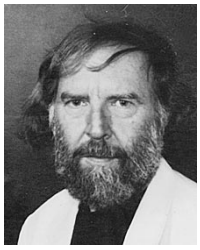

Albert C. van der Woerd was born in Leiden, The Netherlands, in 1937. In 1977, he received the "Ingenieurs" (M.Sc.) degree in electrical engineering from the Delft University of Technology (DUT), Delft, The Netherlands. He received the Ph.D. degree in 1985.

From 1959 to 1966, he was engaged in research on and the development of radar and TV circuits at several industrial laboratories. In 1966, he joined the Electronics Research Laboratory of the Faculty of Electrical Engineering, DUT. For the first 11 years, he carried out research on electronic musical instruments. For the next eight years, his main research subject was carrier domain devices. More recently, he has specialized in the field of low-voltage low-power analog circuits and systems. He teaches design methodology.

Arthur H. M. van Roermund (SM'95) was born in Delft, The Netherlands, in 1951. He received the M.Sc. degree in electrical engineering from the Delft University of Technology (DUT), in 1975 and the Ph.D. degree in applied sciences from the Katholieke Universiteit Leuven, Leuven, Belgium, in 1987.

From 1975 to 1992, he was with the Philips Research Laboratories, Eindhoven, The Netherlands. He first worked in the Consumer Electronics Group on design and integration of analog circuits and systems, especially switched-capacitor circuits. In 1987, he joined the Visual Communications Group, where he was engaged in video architectures and digital video signal processing. From 1987 to 1990, he was Project Leader of the Video Signal Processor Project, and from 1990 to 1992, of a Multi-Window Television Project. Since 1992, he has been a Full Professor, Electrical Engineering Department, DUT, where he is heading the Electronics Research Laboratory. He is also Group Leader of the Electronics Group and coordinator of the circuits and systems section of DIMES: the Delft Institute of Micro Electronics and Submicron technology, which is a cooperation between research groups on microelectronics, technology, and technology-related physics.